

Transmission eigenvalues in random media with surface reflection

Xiaojun Cheng,^{1,2} Chushun Tian,³ and Azriel Z. Genack^{1,2}

¹*Department of Physics, Queens College, The City University of New York, Flushing, NY 11367, USA*

²*The Graduate Center, The City University of New York, New York, NY 10016 USA*

³*Institute for Advanced Study, Tsinghua University, Beijing 100084, China*

(Dated: September 15, 2018)

The impact of surface reflection on the statistics of transmission eigenvalues is a largely unexplored subject of fundamental and practical importance in statistical optics. Here, we develop a first-principles theory and confirm numerically that the distribution of transmission eigenvalues of diffusive waves exhibits a nonanalytic ‘transition’ as the strength of surface reflection at one surface passes through a critical value while that at the other is fixed. Above the critical value, the highest transmission eigenvalue is strictly smaller than unity and decreases with increasing internal reflection. When the input and output surfaces are equally reflective, the highest transmission eigenvalue is unity and the transition disappears irrespective of the strength of surface reflection.

PACS numbers: 42.25.Dd, 42.25.Bs, 71.23.An

The characteristics of transmission through random media are determined by the statistics of the eigenvalues of the transmission matrix. For example, universal conductance fluctuations of diffusive waves are due to correlation between transmission eigenvalues [1], while single parameter scaling of localized waves reflects the dominance in the transmittance of a single transmission eigenvalue with a log-normal distribution [2]. Powerful theoretical methods have been developed to study the statistics of transmission eigenvalues particularly in quasi-one-dimensional disordered waveguides [3–8, 11]. Only recently have measurements of optical [12] and microwave [13] transmission matrices been carried out and have practical applications of the transmission matrix in optical communications and imaging appeared to be feasible [12, 14, 15].

For diffusive waves in quasi-one-dimensional samples, the transmission eigenvalues exhibit a bimodal distribution [4, 6, 7, 11, 16, 17],

$$\rho_0(\mathcal{T}) = \frac{\xi}{2L} \frac{1}{\mathcal{T}\sqrt{1-\mathcal{T}}}. \quad (1)$$

and depends only upon the parameter ξ/L (see Ref. [18] for a review of the early status of this distribution). Here L is the sample length and ξ is the localization length [19]. The distribution of transmission eigenvalues is also bimodal in higher dimensional diffusive samples [17]. Although Eq. (1) was originally predicted for electronic diffusive waves [6], it applies equally to classical waves such as light, sound, and microwave radiation since it arises from coherent wave scattering.

The bimodal distribution was derived with reference to electronic conductors coupled to ideal leads. Additional aspects of random samples are encountered in measurements of the transmission, such as reflective interfaces (e.g., due to a mismatch in refractive index at the boundaries) and absorption or amplification of radiation. Understanding how these additional factors affect the statis-

tics of transmission eigenvalues and the resultant transmission through random systems will deepen our understandings of wave propagation in open complex media and may guide efforts to manipulate transmission for various applications by exciting selected eigenchannels. The statistics of transmission is also affected by experimental considerations such as the inability to measure the full transmitted field for all incoming and outgoing channels [20] which has so far precluded the observation of the bimodal distribution [12, 13].

The average transmission in the presence of internal reflection has been studied [21–23] using the diffusion model or radiative transfer theory [24–26]. The impact of internal reflection on the average intensity has been accounted for in a diffusion model. In this model, the intensity inside the sample is found by solving the diffusion equation in a region extending beyond the physical sample on each side by a length z_b at which the intensity within the sample extrapolates to zero [21–23, 27]. In a sample with internal reflection R , which may arise from the mismatch in refractive indices at the interface, $z_b = 0.7\ell(1+R)/(1-R)$ with mean free path ℓ [21–23]. One might conjecture that the effect of surface reflection upon the distribution of transmission eigenvalues could be accounted for by replacing L by the effective sample length $L + 2z_b$ in Eq. (1). Whether the hypothesis is valid has not been explored. It is clear however that the replacement: $L \rightarrow L + 2z_b$ cannot be generalized to localized waves.

Random matrix techniques [4, 5, 7] are strictly valid in quasi one dimensions, but not in high dimensions (e.g., the slab sample commonly used). Though the Green’s function approach used to derive the bimodal distribution [17] is not restricted to low dimensions, it cannot be easily extended to localized waves. Most importantly, it is unclear how to include surface reflection in these techniques. Recently, a powerful supersymmetric field theory has been developed for classical wave propagation

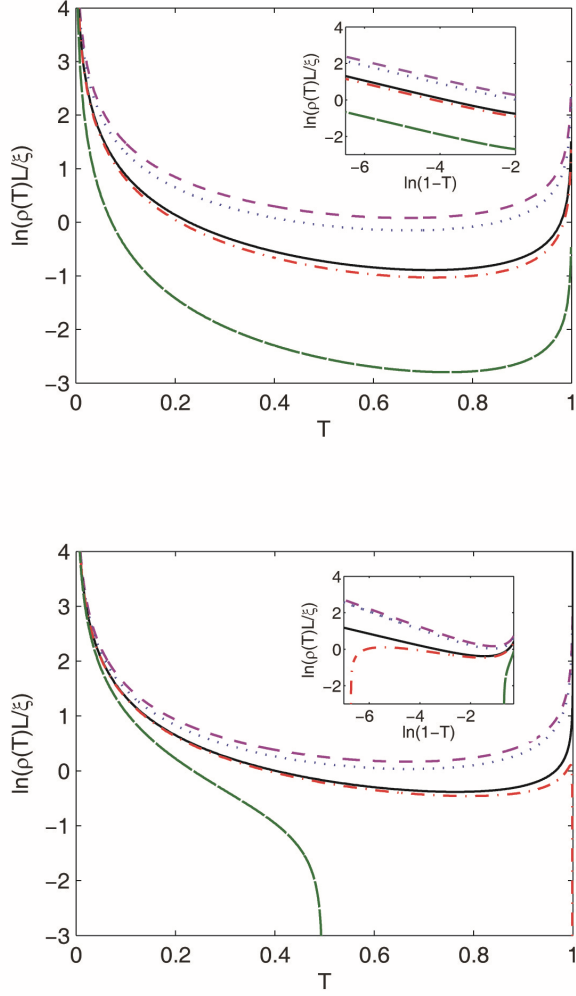


FIG. 1. The analytical theory shows that as the internal reflection on the output surface increases, $\rho(\mathcal{T})$ undergoes an ‘abrupt’ change (‘transition’) at $\zeta = 1$ (lower panel). This transition disappears when the internal reflection is the same on the input and output surfaces (upper panel). The values of ζ are 0.1, 0.25, 1, 1.2, and 8 from top to bottom. Inset: we re-plot the curves in the main panels in ln-ln scale.

[2, 28] and has provided an exact local diffusion theory for localized waves in open random media [2, 30, 31]. The theory is valid for both diffusive and localized waves, and applies to the slab as well as the quasi-one-dimensional geometries. However, the challenging issue of the impact of surface reflection on wave transport in open random media has not been addressed by supersymmetric field theory so far.

In this Letter, we use supersymmetric field theory to demonstrate that wave interference leads to a nonanalytic ‘transition’ of the distribution of transmission eigenvalues as the internal reflection at one surface passes through a critical value while that at the other is fixed. Above the critical value, the highest transmission eigen-

value is strictly smaller than unity and decreases with increasing internal reflection. When input and output surfaces are equally reflective, the highest transmission eigenvalue is unity and the transition disappears irrespective of the strength of surface reflection. We find that although the distribution density for high transmission eigenvalues is completely suppressed by strong internal reflection at the input surface, surprisingly, it is substantially enhanced by adding an identical reflector to the output.

We calculate the transmission eigenvalue distribution, $\rho(\mathcal{T})$, for diffusive samples where $\ell \ll L \ll \xi$. Because of numerous calculational subtleties, we first summarize the main results. We express the deviation from Eq. (1) via the factor $f(\mathcal{T}) \equiv \frac{\rho(\mathcal{T})}{\rho_0(\mathcal{T})}$. When the surface internal reflection R is the same on the input and output surfaces, f is found implicitly from $(\mathcal{T} \equiv \cosh^{-2} \frac{\phi}{2})$

$$\phi = 2 \operatorname{arccosh} \frac{\pi \zeta f}{\cos \frac{\pi f}{2}} + \frac{\sin \frac{\pi f}{2}}{\zeta} \sqrt{\left(\frac{\pi \zeta f}{\cos \frac{\pi f}{2}} \right)^2 - 1}, \quad (2)$$

where the parameter $\zeta \equiv z_b/L$. Equation (2) yields a family of curves of $\rho(\mathcal{T})$ for different values of ζ , which are shown in the upper panel of Fig. 1. When only the output surface is reflective, f is found from

$$\phi = \operatorname{arccosh} \frac{\pi \zeta f}{\sin \pi f} - \frac{\cos \pi f}{\zeta} \sqrt{\left(\frac{\pi \zeta f}{\sin \pi f} \right)^2 - 1}. \quad (3)$$

The plots for different values of internal reflection are shown in the lower panel of Fig. 1. Equations (2) and (3) show that $f(\mathcal{T})$ is governed by a single parameter ζ .

For weak surface interactions, $z_b \ll L$, the two cases are qualitatively similar: Equations (2) and (3) both reduce to $f(\mathcal{T}) = L/L_{\text{eff}}$. (Note that such uniform suppression breaks down for small \mathcal{T} , as required by the normalization.) Here the effective sample length L_{eff} is $(L + 2z_b)$ when the input and output surfaces are equally reflective and $(L + 0.7\ell + z_b)$ when only the output surface is reflective. In the latter case, 0.7ℓ arises from the transparent input surface and z_b from the reflective output surface [24]. As expected, the distribution $\rho(\mathcal{T})$ for relatively transparent samples differs from Eq. (1) only by the overall factor, i.e., $\xi/L \rightarrow \xi/L_{\text{eff}}$.

TABLE I. Asymptotic behavior of $\rho(\mathcal{T})$ at $\mathcal{T} \rightarrow 1$.

location of internal reflection	input and output surface	input or output surface
$\zeta < 1$	$\sim (1 - \mathcal{T})^{-\frac{1}{2}}$	$\sim (1 - \mathcal{T})^{-\frac{1}{2}}$
$\zeta = 1$		$\sim (1 - \mathcal{T})^{-\frac{1}{3}}$
$\zeta > 1$		0

For strong surface interactions, $z_b \gtrsim L$, the deviations from the bimodal distribution are very different for the two cases, as shown in Fig. 1 and as summarized in Table I. In the case of internal reflection only at a single interface, the asymptotic behavior of $\rho(\mathcal{T})$ for $\mathcal{T} \rightarrow 1$ undergoes an abrupt change ('transition') as ζ passes through unity: the singularity of $\rho(\mathcal{T} \rightarrow 1)$ changes from $(1 - \mathcal{T})^{-\frac{1}{2}}$ for $\zeta > 1$ to $(1 - \mathcal{T})^{-\frac{1}{3}}$ for $\zeta = 1$, while $\rho(\mathcal{T} > \mathcal{T}_{\max}) = 0$ for $\zeta > 1$. The highest transmission eigenvalue \mathcal{T}_{\max} decreases with ζ and $\mathcal{T}_{\max} \sim \zeta^{-1}$ for $\zeta \gg 1$. The same results are found when internal reflection is present only at the input instead of the output interface. The transition, however, does not occur when both surfaces are equally reflective. In this case, as internal reflection increases, the asymptotic behavior does not change, i.e., $\rho(\mathcal{T} \rightarrow 1) \sim (1 - \mathcal{T})^{-\frac{1}{2}}$, aside from an overall factor.

The behavior of $f(\mathcal{T})$ predicted by Eq. (3) is confirmed in numerical experiments on wave transport through disordered waveguides using the recursive Green's function method. A scalar wave is launched into a diffusive sample with $\xi/L \approx 16$, which is an 1800×600 rectangular lattice. The lattice spacing is unity (in units of the inverse wavenumber) with the wave velocity in the surrounding air set to unity. The squared refractive index at each site fluctuates independently around the air background value, taking random values over the interval $[0.7, 1.3]$. To create internal reflection, we add an additional layer of thickness 2 lattice spacings and constant refractive index at the output of the sample. Simulations were carried out for refractive indices of the surface layer of 1.8, 2, 2.1, 2.2, and 2.5. For each of these values, we found the 200 transmission eigenvalues in 3,000 disordered configurations. The results, shown in Fig. 2, are in good agreement with the analytical results of Eq. (3). ζ is treated as the single fitting parameter and is found to be 0.16, 0.93, 2.2, 4.0, and 17.2 from top to bottom. Note that the appearance of data points giving nonzero density above \mathcal{T}_{\max} is due to finite channel number in numerical experiments.

If the internal reflection at the input surface is fixed at some nonzero value, the transition still occurs as the internal reflection at the output surface passes through a certain critical value whose detailed form [see Supplementary Materials (SM)] depends on the internal reflection at the input surface. Therefore, it is a large imbalance in the internal reflection at the input and output surfaces that leads to $\mathcal{T}_{\max} < 1$. Importantly, although $\rho(\mathcal{T} \geq \mathcal{T}_{\max}) = 0$ for strong internal reflection on the input surface (the $\zeta = 8$ curve in Fig. 1, lower panel), surprisingly, $\rho(\mathcal{T})$ for high values of \mathcal{T} is substantially enhanced when we add an identical reflector to the output (the $\zeta = 8$ curve in Fig. 1, upper panel). This implies that for $\mathcal{T}_{\max} < 1$ wave functions are sensitive to the boundary conditions and thereby must be delocalized. Thus, this result is a coherent effect for diffusive waves and is related to neither weak nor strong local-

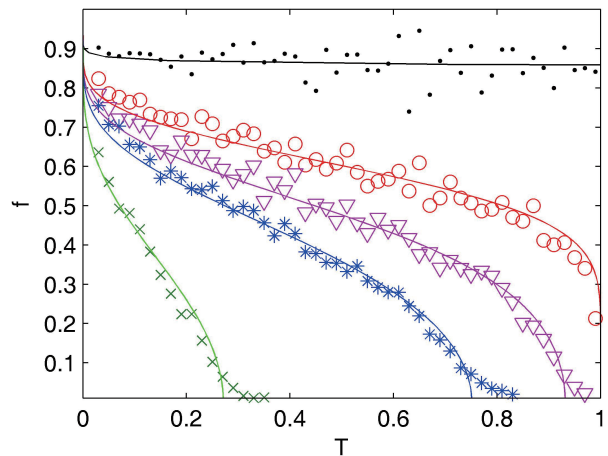


FIG. 2. The numerical results and the analytic prediction of Eq. (3) are in good agreement. This confirms the transition in the transmission eigenvalue statistics. The fit with the single parameter ζ gives $\zeta = 0.16, 0.93, 2.2, 4.0$, and 17.2 from top to bottom.

ization. Rather, it resembles a well-known quantum mechanical phenomenon. That is, although a single barrier prohibits wave transmission, when an identical barrier is added, the system can be perfectly transmitting. Eq. (3) coincides with a result for a completely different context [17, 32], in which a normal metal is coupled to another normal metal or to a superconductor via a *single* barrier. However, the transition here has nothing to do with the localization-delocalization transition of the wave function suggested in Ref. [17], as shown above. Indeed, we use the analytical result of $\rho(\mathcal{T})$ (Fig. 1, lower panel) to numerically compute $\int_0^1 d\mathcal{T} \mathcal{T} \rho(\mathcal{T})$ namely the average conductance (see SM for details). We find that for ζ ranging from 10^{-1} to 10^3 , the average conductance is ξ/L_{eff} , i.e., Ohm's law is valid no matter whether internal reflection is weak or strong.

Having summarized the main results, let us present an outline of the microscopic theory. Because the results above are valid irrespective of time-reversal symmetry, for simplicity we focus on unitary systems for which this symmetry is broken. We start from the case of identical values of internal reflection on the input and output surfaces. The transmission eigenvalue density may be obtained from the function $F(\phi) \equiv -\frac{i}{2} \sinh \phi \langle \text{tr}[\mathbf{t} \mathbf{t}^\dagger / (1 + \sinh^2(\phi/2) \mathbf{t} \mathbf{t}^\dagger)] \rangle$ since $\rho(\mathcal{T}) = \frac{1}{2\pi} [F(\phi + i\pi) + F^*(\phi + i\pi)] \frac{d\phi}{d\mathcal{T}}$, where ϕ is understood as $\phi - i\delta$ with δ a positive infinitesimal, and $\langle \dots \rangle$ represents the average over Gaussian disorder. The function $F(\phi)$ can be cast into a functional integral over the supersymmetric field $Q(x)$ (see Ref. [2] for a review of the applications of supersymmetric field theory [1] to classical waves in open random media). Details of the calculation are presented in SM.

We find

$$F(\phi) = -\frac{i\xi}{2} \int_{(2z_b Q \partial_x Q + [Q, \Lambda])|_{x=0}=0}^{(2z_b Q \partial_x Q - [Q, \Gamma])|_{x=L}=0} D[Q] \times (Q \partial_x Q)_{\text{bb}}^{21}|_{x=0, \theta=i\phi} e^{-\frac{\xi}{8} \int_0^L dx \text{str}(\partial_x Q)^2}, \quad (4)$$

where ‘str’ is the supertrace. Q is a 4×4 supermatrix defined on both the advanced-retarded (‘ar’) and the fermionic-bosonic (‘fb’) sector. More precisely, $Q = T^{-1} \Lambda T$ and the supermatrix T takes the supermatrix value from the coset space $U(1, 1|2)/U(1|1) \otimes U(1|1)$. The crucial difference between Eq. (4) and the expression for disordered electronic wires coupled to ideal leads given in Refs. [3, 4, 11] is the radiative boundary condition at the interfaces, $x = 0, L$ [2, 28]. In Eq. (4), Λ and Γ are constant supermatrices. The former is $\text{diag}(\mathbb{1}^{\text{fb}}, -\mathbb{1}^{\text{fb}})^{\text{ar}}$ and the latter is

$$\text{diag} \left(\begin{pmatrix} \cos \theta & -i \sin \theta \\ i \sin \theta & -\cos \theta \end{pmatrix}^{\text{ar}}, \begin{pmatrix} \cosh \phi & \sinh \phi \\ -\sinh \phi & -\cosh \phi \end{pmatrix}^{\text{ar}} \right)^{\text{fb}},$$

where $0 < \theta < \pi$ and $\phi > 0$.

The functional integral in Eq. (4) is dominated by fluctuations around field configurations which solve the saddle point equation $\partial_x(Q \partial_x Q) = 0$ implemented with the radiative boundary conditions, i.e., $(2z_b Q \partial_x Q + [Q, \Lambda])|_{x=0} = 0$ and $(2z_b Q \partial_x Q - [Q, \Gamma])|_{x=L} = 0$. The solution of $Q(x)$ has the same structure as Γ except for the replacements: $\phi \rightarrow \Phi(x), \theta \rightarrow \Theta(x)$. Substituting these into the saddle point equation and the boundary conditions gives

$$\partial_x^2 \Phi = \partial_x^2 \Theta = 0, \quad (5)$$

satisfying the boundary conditions, i.e.,

$$z_b \partial_x \Phi - \sinh \Phi = z_b \partial_x \Theta - \sin \Theta = 0, \quad (6a)$$

for $x = 0$ and

$$z_b \partial_x \Phi + \sinh(\Phi - \phi) = z_b \partial_x \Theta + \sin(\Theta - \theta) = 0, \quad (6b)$$

for $x = L$. The solution has the form $\Phi(x) = C_\phi x/L + \phi_0$, $\Theta(x) = C_\theta x/L + \theta_0$, where $C_{\phi, \theta} \in \mathbb{R}$, $\phi_0 > 0$ and $0 < \theta_0 < \pi$. It is well defined for arbitrary z_b and converges to the limiting case of $z_b = 0$ [4]. As a result (see SM for derivations),

$$\zeta C_\phi = -\sinh \frac{C_\phi - \phi}{2}, \quad \zeta C_\theta = -\sin \frac{C_\theta - \theta}{2} \quad (7)$$

once ϕ_0 and θ_0 are eliminated from Eqs. (6a) and (6b).

Upon substituting $\Phi(x), \Theta(x)$ into the action $\frac{\xi}{8} \int_0^L dx \text{str}(\partial_x Q)^2$, we find the saddle point action $\sim \frac{\xi}{L} (C_{\theta=i\phi}^2 + C_\phi^2)$. A set of saddle point actions results since the second equation in (7) has a family of solutions. Taking the analytic continuation of the second equation in (7), we find $C_{\theta=i\phi} = iC_\phi$. As a result, the smallest saddle point action is zero, and is gapped from the

others by an action $\sim \mathcal{O}(\frac{\xi}{L})$. Since we are interested in diffusive samples, $\xi/L \gg 1$, we need to consider only the saddle point configuration leading to a vanishing action and fluctuations around this. Upon integrating out fluctuations, a functional superdeterminant which is unity at $\theta = i\phi$ results, thanks to the supersymmetry. We thereby obtain $F(\phi) = -\frac{i}{2} \frac{\xi}{L} C_\phi$. [In deriving this result we ignore fluctuations in the pre-exponential factor of Eq. (4) since they only give rise to corrections of lower order.]

Supposing $z_b = 0$, (This limit, however, cannot be obtained in reality since $z_b \geq 0.7\ell$ [24].) Eq. (5) can be easily solved, giving $C_\phi = \phi$. As a result, $F(\phi) = -\frac{i}{2} \frac{\xi}{L} \phi$. From this, we obtain $\rho(\mathcal{T}) = \frac{\xi}{2L} \frac{d\phi}{d\mathcal{T}}$, namely the bimodal distribution (1). Thus, it is clear that this distribution excludes interface effects. For weak internal reflection, $\zeta \ll 1$, we may expand the sinh and sine functions in Eqs. (7) near zero. Keeping the expansion up to first order, we obtain $f \equiv (C_{\phi+i\pi} - C_{\phi-i\pi})/(2i\pi) = L/L_{\text{eff}}$ with $L_{\text{eff}} = L + 2z_b$. This gives the distribution which is essentially the same as (1) except for the replacement $L \rightarrow L_{\text{eff}}$. This same substitution gives the average transmission in the case of weak internal reflection [21–23, 26]. We see that the effective role of weak internal reflection indeed is to extend the sample length by $2z_b$.

Using the first equation in (7), we can prove Eq. (2) (see SM for details). Setting $\phi = 0$ in Eq. (2), we obtain $\pi \zeta f(1) = \cos \frac{\pi f(1)}{2}$. This equation for $f(1)$ has a unique solution in the interval $(0, 1)$ for arbitrary ζ . Thus, $\rho(\mathcal{T} \rightarrow 1) = \frac{\xi}{2L} \frac{f(1)}{\sqrt{1-\mathcal{T}}}$, i.e., the amplitude of the peak of the distribution (1) as $\mathcal{T} \rightarrow 1$ is suppressed, but the square-root singularity does not change.

We now repeat the procedure above for the case in which only the output surface ($x = L$) is reflective. The key difference is that Eq. (7) is replaced by

$$\zeta C_\phi = -\sinh [(1 + 0.7\ell/L) C_\phi - \phi], \quad (8a)$$

$$\zeta C_\theta = -\sin [(1 + 0.7\ell/L) C_\theta - \theta]. \quad (8b)$$

For $\zeta \ll 1$, we find $\rho(\mathcal{T}) = \frac{\xi}{2L_{\text{eff}}} \frac{1}{\mathcal{T}\sqrt{1-\mathcal{T}}}$ with $L_{\text{eff}} = L + 0.7\ell + z_b$. Again we see that the impact of weak internal reflection ($\zeta \ll 1$) is to extend the sample length: 0.7ℓ is the extension on the transparent input surface and z_b on the reflective output surface. In general, using Eq. (8a), we are able to prove Eq. (3) (see SM for details). For $\zeta < 1$, we have $\rho(\mathcal{T} \rightarrow 1) = \frac{\xi}{2L} \frac{f(1)}{\sqrt{1-\mathcal{T}}}$ as we found above, and the coefficient $f(1)$ now satisfies $\pi \zeta f(1) = \sin \pi f(1)$. For $\zeta = 1$, we obtain from Eq. (3) $\phi \sim f^3$ for $\phi \rightarrow 0$, giving distinct singularity, $\rho(\mathcal{T} \rightarrow 1) \sim (1 - \mathcal{T})^{-\frac{1}{3}}$. For $\zeta > 1$, we find from Eq. (3) that ϕ corresponding to \mathcal{T}_{max} is $\text{arccosh } \zeta - \sqrt{1 - \zeta^{-2}}$. This gives

$$\mathcal{T}_{\text{max}} = \frac{2}{1 + \zeta \cosh \sqrt{1 - \zeta^{-2}} - \sqrt{\zeta^2 - 1} \sinh \sqrt{1 - \zeta^{-2}}}. \quad (9)$$

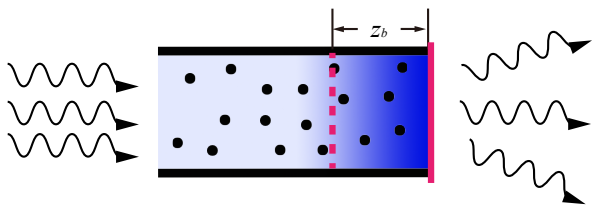


FIG. 3. A resonant cavity formed by internal reflection at the output surface (red solid line) and the ‘virtual’ reflector (red dashed line) formed by scatterers inside the medium. The latter is placed at a distance of z_b from the output surface.

For $\zeta \gg 1$, $\mathcal{T}_{\max} = 2e/\zeta$. In SM, we show further that if the input surface is reflective, the transition may occur also when the internal reflection at the output surface passes a certain critical value, at which z_b at the output surface equals the sum of z_b at the input surface and L .

We consider a possible qualitative physical picture for the transition. We suppose that internal reflection appears only on the output surface. Waves that flow from the input to the output surface are reinjected into the sample as they reflect from the output surface. These waves propagate diffusively over a typical distance z_b , as implied by the boundary constraint for the Q field, which encodes information on the spatial variation of the intensity. The plane which is located inside the medium and at a distance z_b from the output surface may be viewed as a virtual reflector (see Fig. 3). A ‘virtual’ resonant cavity is thereby formed giving rise to perfect transmission. (The same arguments apply if the input surface is reflective instead.) For large internal reflection, $\zeta \geq 1$, the virtual reflector falls outside the medium, and perfect transmission would no longer be possible.

In summary, we have developed a supersymmetric field theory to study the impact of surface interaction on the transmission eigenvalue statistics in random media with arbitrary strength of disorder. Although we focused here on quasi-one-dimensional systems and weak disorder, the theory is also applicable to study the impact of surface reflection in higher dimensions and strongly disordered environments. The analytical calculations of the transition in the distribution of high transmission eigenvalues as the internal reflection at the output surface increases are confirmed numerically. The results are coherent effects for diffusive waves that emerge from the wave nature of propagation but are unrelated to weak localization. They are therefore relevant to transmission in other wave systems in a variety of applications such as, for example, thermal phonon transport in dissimilar solids [34] where effects of surface reflection such as the Kapitza resistance are not negligible.

We would like to thank Zhou Shi for advice on the simulation program and Leonid I. Glazman for useful discussions. This work is supported by the NSF (No.

DMR-1207446), by the NSFC (No. 11174174) and by the Tsinghua University ISRP (No. 2011Z02151).

-
- [1] Y. Imry, *Europhys. Lett.* **1**, 249 (1986).
 - [2] P. W. Anderson, D. J. Thouless, E. Abrahams, and D. S. Fisher, *Phys. Rev. B* **22**, 3519 (1980).
 - [3] M. E. Gertsenshtein, and V. B. Vasil'ev, *Teor. Veroyatn. Primen.* **4**, 424 (1959); **5**, 3(E) (1959) [*Theor. Probab. Appl.* **4**, 391 (1959); **5**, 340(E) (1959)].
 - [4] O. N. Dorokhov, *Pis'ma Zh. Eksp. Teor. Fiz.* **36**, 259 (1982) [*JETP Lett.* **36**, 318 (1982)].
 - [5] O. N. Dorokhov, *Zh. Eksp. Teor. Fiz.* **85**, 1040 (1983) [*Sov. Phys. JETP* **58**, 606 (1983)].
 - [6] O. N. Dorokhov, *Solid State Commun.* **51**, 381 (1984).
 - [7] P. A. Mello, P. Pereyra, and N. Kumar, *Ann. Phys. (N.Y.)* **181**, 290 (1988).
 - [8] K. M. Frahm, *Phys. Rev. Lett.* **74**, 4706 (1995).
 - [9] B. Rejaei, *Phys. Rev. B* **53**, R13235 (1996).
 - [10] A. Lamacraft, B. D. Simons, and M. R. Zirnbauer, *Phys. Rev. B* **70**, 075412 (2004).
 - [11] A. Altland, A. Kamenev, and C. Tian, *Phys. Rev. Lett.* **95**, 206601 (2005).
 - [12] S. M. Popoff *et al.*, *Phys. Rev. Lett.* **104**, 100601 (2010).
 - [13] Z. Shi and A. Z. Genack, *Phys. Rev. Lett.* **108**, 043901 (2012).
 - [14] I. M. Vellekoop and A. P. Mosk, *Phys. Rev. Lett.* **101**, 120601 (2008).
 - [15] A. P. Mosk, A. Lagendijk, G. Leroosey, and M. Fink, *Nat. Photon.* **6**, 283 (2012).
 - [16] P. A. Mello and J.-L. Pichard, *Phys. Rev. B* **40**, 5276 (1989).
 - [17] Yu. V. Nazarov, *Phys. Rev. Lett.* **73**, 134 (1994).
 - [18] C. W. J. Beenakker, *Rev. Mod. Phys.* **69**, 731 (1997).
 - [19] K. B. Efetov and A. I. Larkin, *Zh. Eksp. Teor. Fiz.* **85**, 764 (1983) [*Sov. Phys. JETP* **58**, 444 (1983)].
 - [20] A. Goetschy and A. D. Stone, arXiv:1304.5562.
 - [21] A. Lagendijk, B. Vreeker, and P. de Vries, *Phys. Lett. A* **136**, 81 (1989).
 - [22] J. X. Zhu, D. J. Pine, and D. A. Weitz, *Phys. Rev. A* **44**, 3948 (1991).
 - [23] J. H. Li, A. A. Lisyansky, T. D. Cheung, D. Livdan, and A. Z. Genack, *Europhys. Lett.* **22**, 675 (1993).
 - [24] P. M. Morse and H. Feshbach, *Methods of Theoretical Physics* (McGraw-Hill, New York, N.Y. 1963).
 - [25] S. Chandrasekhar, *Radiative Transfer* (Dover, New York, 1960).
 - [26] M. C. W. van Rossum and Th. M. Nieuwenhuizen, *Rev. Mod. Phys.* **71**, 313 (1999).
 - [27] This entails the standard terminology namely the extrapolation length for z_b . However, this is very misleading in many contexts. For example, for localized waves, the definition of z_b in the diffusion model or radiative transfer theory is meaningless because these theories cease to work. Instead, it has been found [2, 28] that in the field theory of localization in open media, exactly the same relation, $z_b = 0.7\ell(1 + R)/(1 - R)$, enters into the boundary condition satisfied by the field. For diffusive waves, the field-theoretic boundary condition is equivalent to that in the diffusion model or radiative transfer theory.
 - [28] C. Tian, *Phys. Rev. B* **77**, 064205 (2008).

- [29] C. Tian, *Physica E* **49**, 124 (2013).
 [30] C. S. Tian, S. K. Cheung, and Z. Q. Zhang, *Phys. Rev. Lett.* **105**, 263905 (2010).
 [31] L. Y. Zhao, C. S. Tian, Z. Q. Zhang, and X. D. Zhang, arXiv: 1304.0516.
 [32] C. W. J. Beenakker, B. Rejaei, and J. A. Melsen, *Phys. Rev. Lett.* **72**, 2470 (1994).
 [33] K. B. Efetov, *Supersymmetry in Disorder and Chaos* (Cambridge University, Cambridge, England, 1997).
 [34] W. A. Little, *Can. J. Phys.* **37**, 334 (1959).

Supplementary materials for:

Transmission eigenvalues in random media with surface reflection

Xiaojun Cheng,^{1,2} Chushun Tian,³ and Azriel Z. Genack^{1,2}

¹*Department of Physics, Queens College, City University of New York, Flushing, New York 11367, USA*

²*The Graduate Center, The City University of New York, New York, NY 10016 USA*

³*Institute for Advanced Study, Tsinghua University, Beijing 100084, China*

We present below derivations of some of the results in this paper.

I. Field theoretic formalism.

We introduce the generating function

$$\mathcal{Z}(\theta, \phi) = \left\langle \frac{\det(1 - \gamma_1 \gamma_2 \mathbf{t} \mathbf{t}^\dagger)}{\det(1 - \zeta_1 \zeta_2 \mathbf{t} \mathbf{t}^\dagger)} \right\rangle, \quad (10)$$

with the parameters $\gamma_1 = \frac{1}{2} \sin \theta$, $\gamma_2 = \tan \frac{\theta}{2}$, $\zeta_1 = \frac{i}{2} \sinh \phi$ and $\zeta_2 = i \tanh \frac{\phi}{2}$. Taking the derivative of \mathcal{Z} with respect to ζ_2 , we find

$$F(\phi) = -\partial_{\zeta_2} \mathcal{Z}|_{\theta=i\phi}. \quad (11)$$

The great advantage of introducing the generating function is that it can be related to the retarded (advanced) Green function, defined as $(\omega_\pm^2 - \hat{H})G_{\omega_\pm}^{R,A}(\mathbf{r}, \mathbf{r}') = \delta(\mathbf{r} - \mathbf{r}')$, which describe wave propagation in random dielectric media on the microscopic level. Here, the wave group velocity (in surrounding air) is set to unity, ω is the circular wave frequency, and $\omega_\pm = \omega \pm i\delta$ with δ positive infinitesimal. The ‘Hamiltonian’ is $\hat{H} \equiv -\nabla^2 - \omega^2 \delta\epsilon(\mathbf{r})$, where $\delta\epsilon$ represents the fluctuations in the dielectric function. We consider two virtual parallel cross sections inside the random medium and the energy current flowing between. The moments of the transmission matrix $\mathbf{t} \mathbf{t}^\dagger$ can then be expressed in terms of the retarded (advanced) Green function via $\text{tr}(\mathbf{t} \mathbf{t}^\dagger)^n = \text{tr}(\hat{j} \delta_L G_{\omega_2}^A \hat{j} \delta_R G_{\omega_2}^R)^n$, where \hat{j} is the energy flux operator, and $\delta_{L(R)}$ restricts the spatial integral on the left (right) cross section. Combined with the identity: $\det(1 - x \mathbf{t} \mathbf{t}^\dagger) \equiv \exp[-\sum_{n=1}^{\infty} \frac{x^n}{n} \text{tr}(\mathbf{t} \mathbf{t}^\dagger)^n]$, this gives: $\det(1 - x \mathbf{t} \mathbf{t}^\dagger) = \det(1 - x \hat{j} \delta_L G_{\omega_2}^A \hat{j} \delta_R G_{\omega_2}^R)$. As a result,

$$\mathcal{Z}(\theta, \phi) = \left\langle \frac{\det(1 - \gamma_1 \gamma_2 \hat{j} \delta_L G_{\omega_2}^A \hat{j} \delta_R G_{\omega_2}^R)}{\det(1 - \zeta_1 \zeta_2 \hat{j} \delta_L G_{\omega_2}^A \hat{j} \delta_R G_{\omega_2}^R)} \right\rangle. \quad (12)$$

The structure of the ratio of two functional determinants invites the application of the supersymmetric technique of Efetov [1]. Procedures for applying this technique to classical waves in open media are reviewed in Ref. [2]. Here, we only outline the scheme. First, we introduce a 4-component supervector $\psi = \{\psi_{\lambda\alpha}\}$, where the index $\lambda = 1, 2$ distinguishes distinct analytic structure of the advanced (retarded) Green function, and $\alpha = f, b$ the fermionic (bosonic) variables. Recall that in this work we ignore time-reversal symmetry. Next, we perform the disorder averaging, which introduces the effective interaction of the supervector field. We then adopt the super-Hubbard-Stratonovich transformation [1] to decouple the interaction, which introduces a 4×4 supermatrix field, Q . After separating the slow and fast modes, we obtain a nonlinear supermatrix σ model. As a result, a general physical observable is expressed in terms of the functional integral over the Q -field which obeys the nonlinear constraint: $Q^2 = 1$. In the last step, we derive the boundary condition satisfied by the Q -field. It is very important that this accounts for the open nature of random media, and retains the distinction in localization physics between open media and infinite (closed) media. As a result,

$$\mathcal{Z}(\theta, \phi) = \int D[Q] e^{-\mathcal{F}[Q]}, \quad \mathcal{F}[Q] = \frac{\xi}{8} \int_0^L dx \text{str}(\partial_x Q - i[\mathcal{A}_x, Q])^2. \quad (13)$$

Here, the ‘gauge field’ $\mathcal{A}_x = \delta_R(\gamma_1 \mathbb{E}_{ff}^{12} \oplus \zeta_1 \mathbb{E}_{bb}^{12}) \oplus \delta_L(\gamma_2 \mathbb{E}_{ff}^{21} \oplus \zeta_2 \mathbb{E}_{bb}^{21})$ which vanishes at the interfaces. $\mathbb{E}_{\alpha\alpha'}^{\lambda\lambda'}$ is a projector which takes the value of unity for the entry $(\lambda\alpha, \lambda'\alpha')$ and is zero otherwise. The supermatrix field is constrained by the boundary condition arising from internal reflection,

$$(2z_b Q \partial_x Q \pm [Q, \Lambda])|_{x=0, L} = 0, \quad (14)$$

where $z_b = 0.7\ell \frac{1+R}{1-R}$ depends on the internal reflection coefficient R at the interface, and the $+$ ($-$) sign corresponds to the left (right) interface located at $x = 0$ ($x = L$). Notice that Eq. (14) is the source of the difference between the present and previous theories [3].

Substituting Eq. (13) into Eq. (11), we find $F(\phi) = -\frac{i}{2}\xi \int D[Q] \text{str}(\delta_L \mathbb{E}_{bb}^{21} Q(\partial_x Q - i[\mathcal{A}_x, Q])) e^{-\mathcal{F}[Q]}|_{\theta=i\phi}$. Notice that the spatial integral included by the supertrace is effectively restricted on the left cross section by δ_L . Making the gauge transformation: $Q(x) \rightarrow S(x)Q(x)S^{-1}(x)$, $S(x) = \text{T}e^{i \int_{-\infty}^x \mathcal{A}_x dx'}$, with ‘T’ denoting the path-ordered product, we obtain Eq. (4).

II. Derivations of Eqs. (7).

The solution of $\Phi(x), \Theta(x)$ must satisfy two conditions: it must be well defined for arbitrary $\zeta \geq 0$ and it must converge to its limiting case at $\zeta = 0$ given e.g., before in Ref. [4]. From the boundary constraints on Φ given in Eqs. (6a) and (6b), we obtain

$$-\sinh \phi_0 = \sinh(C_\phi + \phi_0 - \phi), \quad (15)$$

giving $\phi_0 = -(C_\phi - \phi)/2$. Inserting this back into Eq. (6a) we obtain the first equation of (7).

From the boundary constraints of Θ given in Eqs. (6a) and (6b), we obtain

$$-\sin \theta_0 = \sin(C_\theta + \theta_0 - \theta). \quad (16)$$

There are two possibilities for matching both sides. (i) $(2n+1)\pi + \theta_0 = C_\theta + \theta_0 - \theta$, $n \in \mathbb{N}$ which gives $C_\theta = \theta + (2n+1)\pi$. However, this solution must be discarded because it cannot match the limiting case of $\zeta = 0$, where $C_\theta = \theta + 2n\pi$ [4]. (ii) $-\theta_0 = C_\theta + \theta_0 - \theta - 2n\pi$ which gives

$$\theta_0 = -\frac{C_\theta - \theta}{2} + n\pi. \quad (17)$$

Inserting this back into Eq. (6a) we obtain

$$\zeta C_\theta + \sin\left(\frac{C_\theta - \theta}{2} - n\pi\right) = 0. \quad (18)$$

Suppose that n is odd. It is easy to see that Eq. (18) has a unique real solution for arbitrary $\zeta \geq 0$. In addition, this solution satisfies $0 < \frac{\theta - C_\theta}{2} < \pi$. Because of $0 < \theta_0 < \pi$ Eq. (17) requires $n = 0$. This contradicts the presumed odd parity of n and therefore n must be even. We thereby obtain the second equation of (7). In fact, it is easy to see that the latter has unique real solution for arbitrary $\zeta \geq 0$. In addition, this solution satisfies $0 < \frac{\theta - C_\theta}{2} < \pi$ which implies $n = 0$. Thus, we complete the proof of Eq. (7).

III. Derivations of Eq. (2).

From the first equation of (7) we obtain

$$\zeta C_{\phi_\pm} = -\sinh \frac{C_{\phi_\pm} - \phi_\pm}{2}. \quad (19)$$

For the moment we assume $\phi_\pm > 0$ and set these to $\phi \pm i\pi$ in the final results. From this equation we further obtain

$$\begin{aligned} \zeta(C_{\phi_+} + C_{\phi_-}) &= -2 \sinh \left[\frac{1}{2} \left(\frac{C_{\phi_+} + C_{\phi_-}}{2} - \bar{\phi} \right) \right] \cosh \left(\frac{1}{2} \frac{C_{\phi_+} - C_{\phi_-} - \Delta\phi}{2} \right), \\ \zeta(C_{\phi_+} - C_{\phi_-}) &= -2 \cosh \left[\frac{1}{2} \left(\frac{C_{\phi_+} + C_{\phi_-}}{2} - \bar{\phi} \right) \right] \sinh \left(\frac{1}{2} \frac{C_{\phi_+} - C_{\phi_-} - \Delta\phi}{2} \right). \end{aligned} \quad (20)$$

where $\bar{\phi} \equiv (\phi_+ + \phi_-)/2$, $\Delta\phi \equiv \phi_+ - \phi_-$. These two equations may be rewritten as

$$\begin{aligned} \frac{C_{\phi_+} + C_{\phi_-}}{2} - \bar{\phi} &= -\frac{1}{\zeta} \sinh \left[\frac{1}{2} \left(\frac{C_{\phi_+} + C_{\phi_-}}{2} - \bar{\phi} \right) \right] \cosh \left(\frac{1}{2} \frac{C_{\phi_+} - C_{\phi_-} - \Delta\phi}{2} \right) - \bar{\phi}, \\ \frac{C_{\phi_+} + C_{\phi_-}}{2} - \bar{\phi} &= \pm 2 \operatorname{arccosh} \left[-\frac{\zeta(C_{\phi_+} - C_{\phi_-})/2}{\sinh \left(\frac{1}{2} \frac{C_{\phi_+} - C_{\phi_-} - \Delta\phi}{2} \right)} \right]. \end{aligned} \quad (21)$$

The sign on the right-hand side of the second equation will be determined below. Inserting the second equation into the first gives

$$\pm 2 \operatorname{arccosh} \left[-\frac{\zeta(C_{\phi_+} - C_{\phi_-})/2}{\sinh \left(\frac{1}{2} \frac{C_{\phi_+} - C_{\phi_-} - \Delta\phi}{2} \right)} \right] = \mp \frac{1}{\zeta} \sqrt{\left[\frac{\zeta(C_{\phi_+} - C_{\phi_-})/2}{\sinh \left(\frac{1}{2} \frac{C_{\phi_+} - C_{\phi_-} - \Delta\phi}{2} \right)} \right]^2 - 1} \cosh \left(\frac{1}{2} \frac{C_{\phi_+} - C_{\phi_-} - \Delta\phi}{2} \right) - \bar{\phi} \quad (22)$$

Upon setting $\bar{\phi} = \phi$, $\Delta\phi = 2i\pi$, we have $f(\phi) = (C_{\phi_+} - C_{\phi_-})/(2i\pi)$. Inserting these into Eq. (22), we find

$$\mp \phi = 2 \operatorname{arccosh} \frac{\pi \zeta f}{\cos \frac{\pi f}{2}} + \frac{\sin \frac{\pi f}{2}}{\zeta} \sqrt{\left(\frac{\pi \zeta f}{\cos \frac{\pi f}{2}} \right)^2 - 1}. \quad (23)$$

Because $\phi > 0$ we need to take the positive sign and therefore obtain Eq. (2).

IV. Derivations of Eq. (3).

First of all, thanks to $\ell/L \ll 1$ we may simplify Eqs. (8a) and (8b) to

$$\zeta C_\phi = -\sinh(C_\phi - \phi), \quad (24a)$$

$$\zeta C_\theta = -\sin(C_\theta - \theta). \quad (24b)$$

Then, the procedure is similar to the derivations of Eq. (2). From Eq. (24a) we obtain

$$\zeta C_\pm = -\sinh(C_\pm - \phi_\pm). \quad (25)$$

Here again, we assume for the moment $\phi_\pm > 0$ and set these to $\phi \pm i\pi$ in the final results. From Eq. (25), we obtain

$$\begin{aligned} \zeta(C_{\phi_+} + C_{\phi_-}) &= -2 \sinh \left(\frac{C_{\phi_+} + C_{\phi_-}}{2} - \bar{\phi} \right) \cosh \frac{C_{\phi_+} - C_{\phi_-} - \Delta\phi}{2}, \\ \zeta(C_{\phi_+} - C_{\phi_-}) &= -2 \cosh \left(\frac{C_{\phi_+} + C_{\phi_-}}{2} - \bar{\phi} \right) \sinh \frac{C_{\phi_+} - C_{\phi_-} - \Delta\phi}{2}. \end{aligned} \quad (26)$$

These two equations may be rewritten as

$$\begin{aligned} \frac{C_{\phi_+} + C_{\phi_-}}{2} - \bar{\phi} &= -\frac{1}{\zeta} \sinh \left(\frac{C_{\phi_+} + C_{\phi_-}}{2} - \bar{\phi} \right) \cosh \frac{C_{\phi_+} - C_{\phi_-} - \Delta\phi}{2} - \bar{\phi}, \\ \frac{C_{\phi_+} + C_{\phi_-}}{2} - \bar{\phi} &= \pm \operatorname{arccosh} \left(-\frac{\zeta(C_{\phi_+} - C_{\phi_-})/2}{\sinh \frac{C_{\phi_+} - C_{\phi_-} - \Delta\phi}{2}} \right). \end{aligned} \quad (27)$$

The sign on the right-hand side of the second equation will be determined below. Inserting the second equation into the first gives

$$\pm \operatorname{arccosh} \left(-\frac{\zeta(C_{\phi_+} - C_{\phi_-})/2}{\sinh \frac{C_{\phi_+} - C_{\phi_-} - \Delta\phi}{2}} \right) = \mp \frac{1}{\zeta} \sqrt{\left(\frac{\zeta(C_{\phi_+} - C_{\phi_-})/2}{\sinh \frac{C_{\phi_+} - C_{\phi_-} - \Delta\phi}{2}} \right)^2 - 1} \cosh \frac{C_{\phi_+} - C_{\phi_-} - \Delta\phi}{2} - \bar{\phi}. \quad (28)$$

Setting $\bar{\phi} = \phi$, $\Delta\phi = 2i\pi$, we obtain

$$\mp \phi = \operatorname{arccosh} \frac{\pi \zeta f}{\sin \pi f} - \frac{\cos \pi f}{\zeta} \sqrt{\left(\frac{\pi \zeta f}{\sin \pi f} \right)^2 - 1}. \quad (29)$$

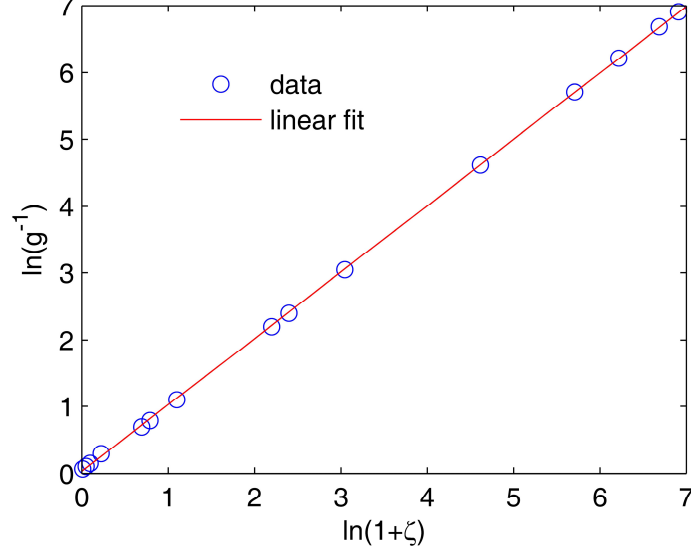


FIG. 4. The average conductance obeys Ohm's law. The data can be fitted to a straight line whose slope is unity.

Because $\phi > 0$ we need to take the positive sign and therefore obtain Eq. (3).

V. Transition for imbalanced internal reflection.

Here we show that if the internal reflection at the input surface, $R_1 > 0$, is fixed and the internal reflection at the output surface, R_2 , increases, the distribution of transmission eigenvalues may also exhibit a transition. For convenience below, we introduce the following parameters: $z_{b1,b2} = 0.7\ell(1 + R_{1,2})/(1 - R_{1,2})$ and $\zeta_{1,2} = z_{b1,b2}/L$. To simplify technical discussions below, we assume ζ_1 small and arbitrary ζ_2 .

For imbalanced internal reflection, $z_{b1} \neq z_{b2}$, the boundary conditions (6a) and (6b) are replaced by

$$(z_{b1}\partial_x\Phi - \sinh\Phi)|_{x=0} = 0, \quad (z_{b2}\partial_x\Phi + \sinh(\Phi - \phi))|_{x=L} = 0. \quad (30)$$

Here, we present only the boundary conditions of $\Phi(x)$ because, as we have seen above, they are sufficient for the purpose of calculating the deviation factor $f(\mathcal{T})$. Inserting the solution to Eq. (6a), i.e., $\Phi(x) = C_\phi x/L + \phi_0$, into Eq. (30), we obtain

$$\zeta_1 C_\phi - \sinh\phi_0 = 0, \quad \zeta_2 C_\phi + \sinh(C_\phi + \phi_0 - \phi) = 0. \quad (31)$$

Because of $\zeta_1 \ll 1$ we may expand the sinh function in the first equation. We then eliminate ϕ_0 to obtain

$$\zeta_2 C_\phi = -\sinh((1 + \zeta_1)C_\phi - \phi). \quad (32)$$

Defining $\tilde{C}_\phi \equiv (1 + \zeta_1)C_\phi$ and $\tilde{\zeta} \equiv \zeta_2/(1 + \zeta_1)$, we rewrite this equation as

$$\tilde{\zeta}\tilde{C}_\phi = -\sinh(\tilde{C}_\phi - \phi). \quad (33)$$

The deviation factor is $f = (\tilde{C}_{\phi+i\pi} - \tilde{C}_{\phi-i\pi})/[2i\pi(1 + \zeta_1)] \equiv \tilde{f}/(1 + \zeta_1)$, and the distribution of transmission eigenvalues is

$$\rho(\mathcal{T}) = \tilde{f}(\mathcal{T}) \times \left[\frac{\xi}{2(L + z_{b1})} \frac{1}{\mathcal{T}\sqrt{1 - \mathcal{T}}} \right]. \quad (34)$$

Now we may repeat the procedure of Sec. IV. As a result, we obtain the same equation as (29) albeit with the replacement: $\zeta \rightarrow \tilde{\zeta}$, $f \rightarrow \tilde{f}$. This implies that the same transition as that discussed in the main text also occurs here. The transition point is $\tilde{\zeta} = 1$, i.e., $z_{b2} = L + z_{b1}$.

VI. Average conductance.

Here we only study the most interesting case in which a single surface is reflective. We first rescale the average conductance by ξ/L . The resultant quantity, denoted as g , is given by

$$g = \frac{1}{2} \int_0^1 d\mathcal{T} \mathcal{T} \times \frac{f(\mathcal{T})}{\mathcal{T}\sqrt{1-\mathcal{T}}} = \frac{1}{2} \int_0^1 d\mathcal{T} \frac{f(\mathcal{T})}{\sqrt{1-\mathcal{T}}}, \quad (35)$$

which depends on a single parameter ζ . We cannot analytically calculate $g(\zeta)$. Rather, we numerically compute it for a wide range of ζ from 10^{-1} to 10^3 . We find that the numerical results for $g(\zeta)$ are well fitted by $1/(1+\zeta)$, as shown in Fig. 4. Therefore, the average conductance is $g(\zeta)\xi/L = \xi/(L+z_b)$. It is important that in spite of the transition exhibited by the distribution $\rho(\mathcal{T})$ at the critical value of $\zeta = 1$, the average conductance obeys Ohm's law for both weak ($\zeta \ll 1$) and strong ($\zeta \gg 1$) internal reflection.

-
- [1] K. B. Efetov, *Supersymmetry in Disorder and Chaos* (Cambridge University, Cambridge, England, 1997).
 - [2] C. Tian, *Physica E* **49**, 124 (2013).
 - [3] B. Rejaei, *Phys. Rev. B* **53**, R13235 (1996).
 - [4] A. Lamacraft, B. D. Simons, and M. R. Zirnbauer, *Phys. Rev. B* **70**, 075412 (2004).
-